

Supplemental Material to Simulations of TiO₂ nanoparticles synthesised off-centreline in jet-wall stagnation flames

Eric J. Bringley, Manoel Y. Manuputty, Casper Lindberg, Gustavo Leon, Jethro Akroyd and Markus Kraft*

*Corresponding author address: mk306@cam.ac.uk

A Governing equations

The governing equations for laminar reacting flow [19, 21] are partial differential equations in space and time, t , which describe the conservation of mass,

$$\frac{\partial \rho}{\partial t} + \nabla \cdot (\rho U) = 0; \quad (\text{A.1})$$

momentum,

$$\frac{\partial \rho U}{\partial t} + \nabla \cdot (\rho U U) = -\nabla p - \mu (\nabla U + (\nabla U)^T); \quad (\text{A.2})$$

species,

$$\frac{\partial \rho Y_i}{\partial t} + \nabla \cdot (\rho U Y_i) + \nabla \cdot (\rho V_i^c Y_i) = \dot{\omega}_i \quad \text{for } i = 1, \dots, N_{\text{sp}}; \quad (\text{A.3})$$

and energy,

$$c_p \frac{\partial \rho T}{\partial t} + c_p \nabla \cdot (\rho U T) = \nabla \cdot (\lambda \nabla T) - \left(\rho \sum_{i=1}^N c_{p,i} Y_i V_i^c \right) \cdot \nabla T + \dot{\omega}_T; \quad (\text{A.4})$$

where ρ is density, U is velocity, Y_i is the mass fraction of species i , T is temperature, p is pressure, V_i^c is the corrected diffusive velocity of species i , $\dot{\omega}_i$ is the mass rate of formation of species i , $\dot{\omega}_T$ is the enthalpy heat release, μ is mixture viscosity, λ is the mixture thermal conductivity, and c_p is the mixture heat capacity.

Transport equations are required to describe the particle phase. Even for particles that are described by a single internal coordinate (*e.g.* particle size, k), an infinite number of transport equations would be required to describe the number of particles of each possible size, making such an approach intractable. In this work, the transport equations to describe the population of univariate, spherical TiO₂ particles are transformed using the method of moments. The particles are assumed to be spherical, have very low volume fraction, have negligible mass, and have no influence on the momentum or enthalpy of the gas-phase. The evolution of the moments of the distribution per unit mass, $\hat{M}_j = \frac{M_j}{\rho}$, is governed by the following transport equation:

$$\frac{\partial \rho \hat{M}_j}{\partial t} + \nabla \cdot (\rho U \hat{M}_j) + \nabla \cdot (\rho V_T \hat{M}_j) = \nabla \cdot \left(\rho D_{p_1} \nabla \hat{M}_{j-\frac{2}{3}} \right) + \dot{\omega}_j \quad \text{for } j = 0, \dots, N_{\text{mom}} - 1. \quad (\text{A.5})$$

In this equation, D_{p_1} is the diffusion coefficient of the smallest particle (of size $k = 1$), V_T is the thermophoretic velocity, and N_{mom} is the number of moments solved for ($N_{\text{mom}} = 6$

in this case). The source terms of the moment equations $\hat{\omega}_j$ include terms describing inception, coagulation and surface growth processes [5, 15]. The source terms and the $\hat{M}_{j-\frac{2}{3}}$ field are unclosed. The equations are closed using interpolative closure (MoMIC) [6].

The ideal (perfect) gas law [1] was additionally used to close the above equations. The heat capacities, $c_{p,i}$; enthalpy, h_i ; and entropy, s_i of species i are described using JANAF polynomials [8]. Mixture-averaged properties are calculated as mass-weighted sums of N_{sp} species with molecular weight W_i . The mixture viscosity is defined by a semi-empirical formula by Wilke [23] that has been modified by Bird et al. [2]:

$$\mu = \sum_{i=1}^{N_{\text{sp}}} \frac{X_i \mu_i}{\sum_{i_2=1}^{N_{\text{sp}}} X_{i_2} \phi_{i,i_2}}, \quad (\text{A.6})$$

where X_i , W_i , and μ_i are the mole fraction, molecular weight, and viscosity of species i , and

$$\phi_{i,i_2} = \frac{1}{\sqrt{8}} \left(1 + \frac{W_{i_1}}{W_{i_2}}\right)^{-\frac{1}{2}} \left(1 + \left(\frac{\mu_{i_1}}{\mu_{i_2}}\right)^{\frac{1}{2}} \left(\frac{W_{i_2}}{W_{i_1}}\right)^{\frac{1}{4}}\right)^2. \quad (\text{A.7})$$

The mixture thermal conductivity is given by Mathur et al. [17]:

$$\lambda = \frac{1}{2} \left(\sum_{i=1}^{N_{\text{sp}}} X_i \lambda_i + \left[\sum_{i=1}^{N_{\text{sp}}} X_i / \lambda_i \right]^{-1} \right), \quad (\text{A.8})$$

where λ_i is the thermal conductivity of species i .

A model is needed to describe the mass flux due to concentration gradients in a multicomponent gas mixture. A mixture-averaged approach [11] is used to calculate a single diffusion coefficient for each species. The binary diffusion coefficient, D_{i,i_2} , given below, is a function of temperature; pressure; the reduced molecular weight, \bar{W}_{i,i_2} ; the reduced collision diameter, σ_{i_2,i_2} ; and a collision integral, $\Omega^{(1,1)*}$ based on reduced temperature [18]:

$$D_{i,i_2} = \frac{3}{16} \frac{\sqrt{2\pi k_B^3 T^3 / \bar{W}_{i,i_2}}}{p \pi \sigma_{i_2,i_2}^2 \Omega^{(1,1)*}}, \quad (\text{A.9})$$

where

$$\bar{W}_{i,i_2} = (W_i^{-1} + W_{i_2}^{-1})^{-1}. \quad (\text{A.10})$$

The mixture-averaged approach of Hirschfelder and Curtiss [10] is used to calculate the mixture diffusion coefficient, D_i . This approach is not inherently mass conserving, so a corrective velocity, V_c , is applied to each species to ensure that mass conservation is followed. The final, corrected diffusion velocity, V_i^c , is the sum of the mass flux and the corrective velocity.

$$D_i = \frac{1 - Y_i}{\sum_{i_2 \neq i}^{N_{\text{sp}}} \frac{X_{i_2}}{D_{i,i_2}}} \quad (\text{A.11})$$

$$V_i^c = V_i + V_c, \quad V_i = -D_i \frac{\nabla X_i}{X_i}, \quad V_c = -\sum_i^{N_{\text{sp}}} Y_i V_i \quad (\text{A.12})$$

The diffusion coefficient of particles of size k due to Brownian motion in the free-molecular regime, D_{p_k} , can be expressed as [7]:

$$D_{p_k} = \frac{3}{2\rho} \left(1 + \frac{\pi\alpha_T}{8}\right)^{-1} \sqrt{\frac{Wk_B T}{2\pi N_A}} \frac{1}{d_k^2}, \quad (\text{A.13})$$

where α_T is a thermal accommodation factor (fraction of gas molecules that leave the surface in equilibrium), N_A is Avagadro's constant, and d_k is the diameter of a particle of size k . The thermal accommodation factor usually takes a value of 0.9 [7]. Under the spherical particle assumption, the diameter of a particle of size k scales by $k^{1/3}$. This can be used to describe D_{p_k} as a function of k and D_{p_1} :

$$\begin{aligned} D_{p_k} &= \frac{3}{2\rho} \left(1 + \frac{\pi\alpha_T}{8}\right)^{-1} \sqrt{\frac{Wk_B T}{2\pi N_A}} \frac{1}{(d_1 k^{1/3})^2} \\ &= \frac{3}{2\rho} \left(1 + \frac{\pi\alpha_T}{8}\right)^{-1} \sqrt{\frac{Wk_B T}{2\pi N_A}} \frac{1}{d_1^2} k^{-2/3} \\ &= D_{p_1} k^{-2/3}. \end{aligned} \quad (\text{A.14})$$

When applying the definition of moments to the infinite number of particle transport equations, the diffusion transport term of moment \hat{M}_j results in the

$$\nabla \cdot \left(\rho D_{p_1} \nabla \hat{M}_{j-\frac{2}{3}} \right)$$

term in Eqn. A.5. The thermophoretic velocity of the particles, V_T , is assumed to be independent of particle size and is expressed as [7]:

$$V_T = -\frac{3}{4} \left(1 + \frac{\pi\alpha_T}{8}\right)^{-1} \frac{\mu}{\rho T} \nabla T. \quad (\text{A.15})$$

V_T acts as an additional convective flux term in Eqn. A.5.

Figure A.1 shows the algorithm used in this work. The algorithm is rooted in the PISO algorithm [13] for handling the velocity-pressure coupling, with the addition of solving scalar fields for chemistry and particle fields. The chemical and moment source terms are calculated by treating each cell as a constant-pressure batch reactor and is solved by integrating the system using ordinary differential equations solvers. The solver is paralised using a domain decomposition method, where the domain is split into smaller domains for each processor to solve for. Adjacent domains are connected using halo cells.

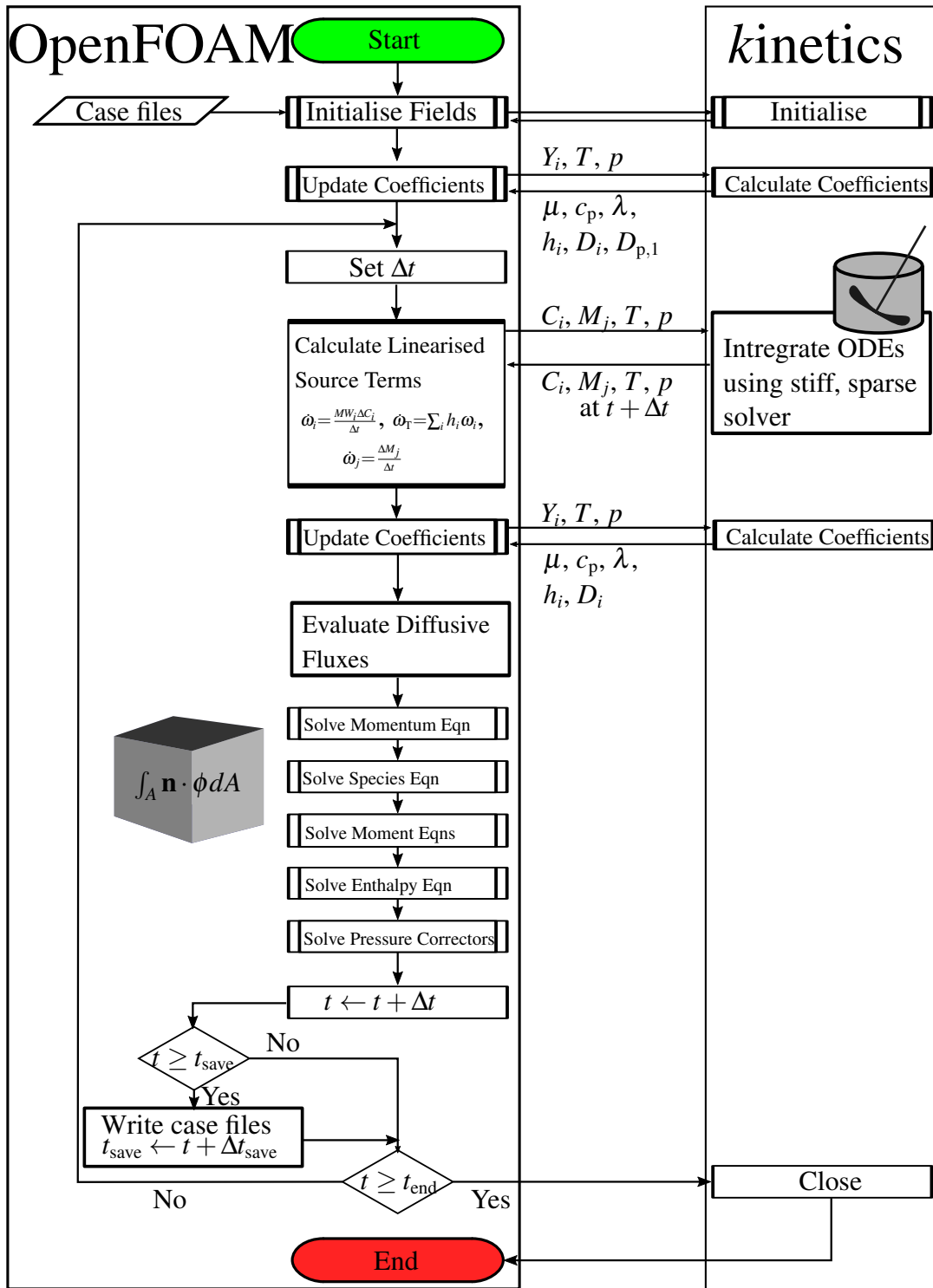


Figure A.1: A diagram of the implemented algorithm. The governing transport equations are solved using OpenFOAM [20] while detailed coefficients and source terms are calculated using kinetics [4].

Table A.1 gives details of all the model parameters.

Table A.1: Model Parameters.

Parameter	Value	Notes
<i>Gas-phase model</i>		
Mechanism	-	UCSD [24] with a reduced mechanism for TTIP decomposition [14]
c_p, h	mixture dependent	JANAF polynomials [8]
μ	mixture dependent	Semi-empirical formula [2, 23]
λ	mixture dependent	Semi-empirical formula [17]
D_i	mixture dependent	Mixture-averaged diffusion [9]
<i>Spherical particle model</i>		
ε	2.64	Collision enhancement factor
$d_{c, \text{Ti(OH)}_4}$	5.128×10^{-10} m	Collision diameter of Ti(OH)_4 [3]
$m_{\text{Ti(OH)}_4}$	115.93 kg kmol ⁻¹	Mass of Ti(OH)_4
α_T	1	Thermal accommodation factor
γ_{IN}	1	Inception efficiency
γ_{SG}	1	Surface growth efficiency
ρ_{TiO_2}	4.25 kg m ⁻³	Density of titania (rutile) [†]
<i>Hybrid particle-number/detailed particle model</i>		
N_{thresh}	100	$d(N_{\text{thresh}}) = 1.8$ nm
α_{crit}	3	Critical sintering exponent [14]
$d_{p, \text{crit}}$	4 nm	Critical sintering diameter [14]
$E_{a, \text{sintering}}$	31030 K	Grain boundary diffusion activation energy
$A_{\text{sintering}}$	2.278×10^{17} s m ⁻⁴ K ⁻¹	Sintering frequency factor
ε	2.64	Collision enhancement factor
γ_{IN}	1	Inception efficiency
γ_{SG}	1	Surface growth efficiency
ρ_{TiO_2}	3.84 kg m ⁻³	Density of titania (anatase) [†]

[†] The densities are taken to be that as suggested by the original publications.

B Assessment of particle size distribution similarity

The similarity of the PSDs are assessed using the two sample Kolmogorov-Smirnov (KS) test [12, 16, 22] for each distribution pair. The null hypothesis, H_0 , was that the two underlying distributions from which the samples were taken are equal.

Figure B.1 presents the results of the two sample KS tests as reject (blue) or fail-to-reject (yellow) the null hypothesis of equivalent distributions. Similar trends are observed in all four cases. The PSDs of trajectories are mostly similar up to a critical radius beyond which the distributions become statistically different. In the lean flame, the critical radius was $r/r_0 \approx 1$ (0.7 cm) for the 280 ppm loading and $r/r_0 \approx 1.5$ (1.1 cm) for the 560 ppm loading. In the stoichiometric flame, the critical radius was $r/r_0 \approx 1$ (0.7 cm) for both TTIP loadings.

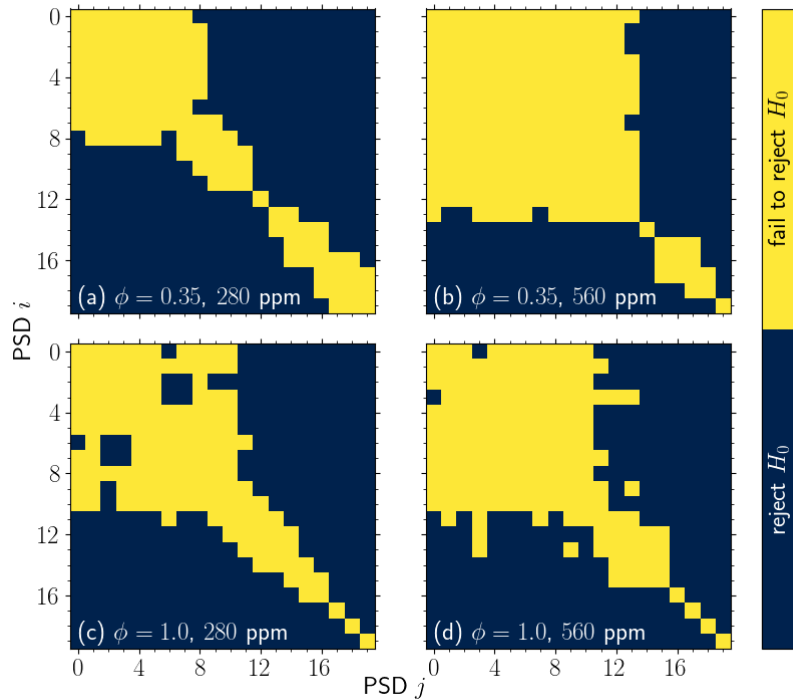


Figure B.1: Results of two sample Kolmogorov-Smirnov test between particle ensembles from different trajectories. The null hypothesis, H_0 , was that the two underlying distributions from which the samples were taken are equal. Results marked with yellow fail to reject H_0 : the two distributions are equal at the $\alpha = 0.01$ confidence level; results marked with blue provide evidence to reject H_0 ($p < 0.005$).

C Additional figures

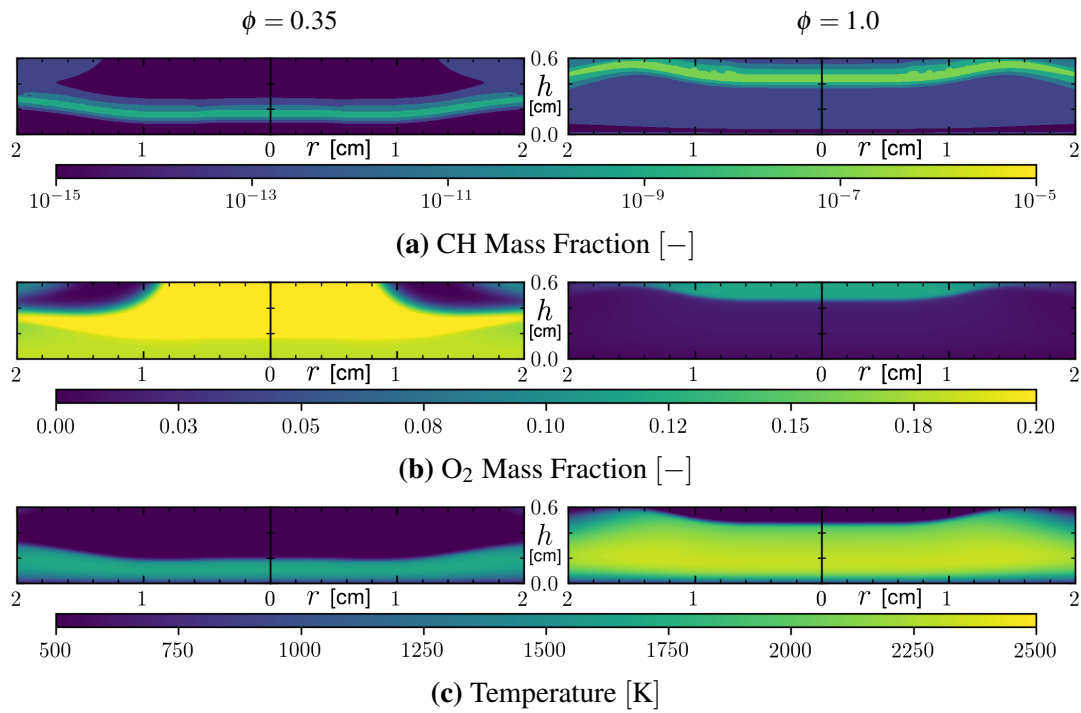


Figure C.1: 2D mass fraction and temperature fields for the $\phi = 0.35$ (left) and $\phi = 1.0$ (right) flames without TTIP.

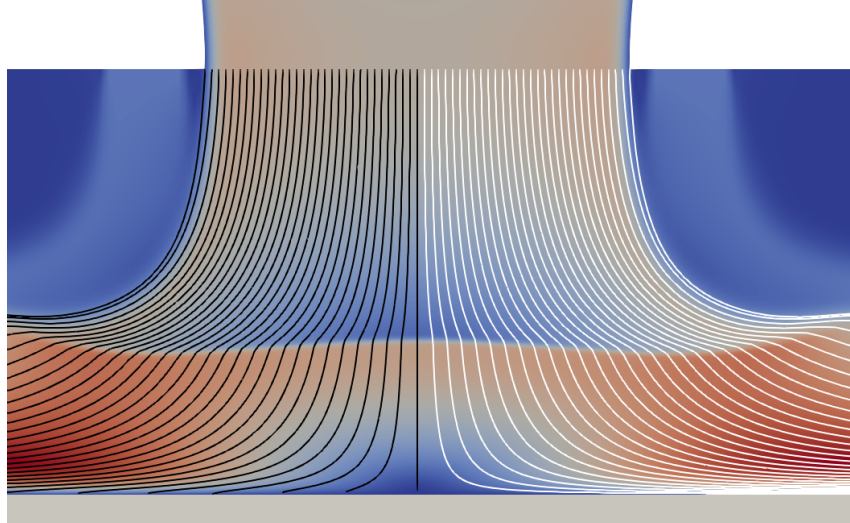


Figure C.2: Trajectories with (left) and without (right) thermophoretic drift. The trajectories that include thermophoretic drift impinge on the stagnation plate whereas trajectories without it do not.

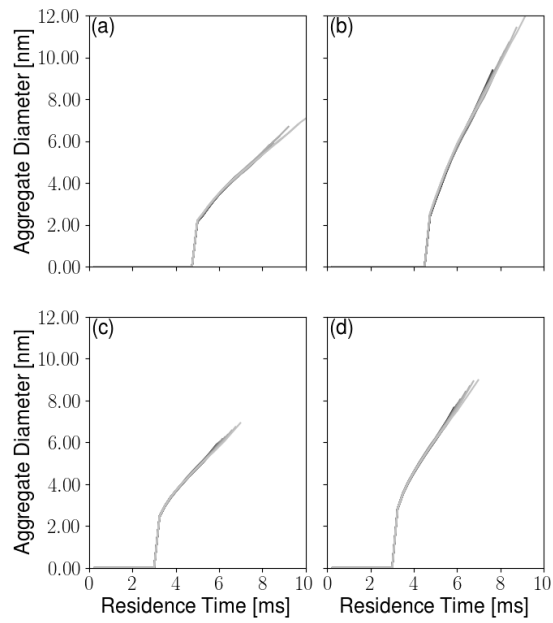


Figure C.3: Mean aggregate diameter as a function of residence time along different trajectories (dark to light moving radially outwards from the centre of the flame) in (a) $\phi = 0.35$, 280 ppm flame, (b) $\phi = 0.35$, 560 ppm flame, (c) $\phi = 1.0$, 280 ppm flame, and (d) $\phi = 1.0$, 560 ppm flame. The inception mode is excluded in this figure.

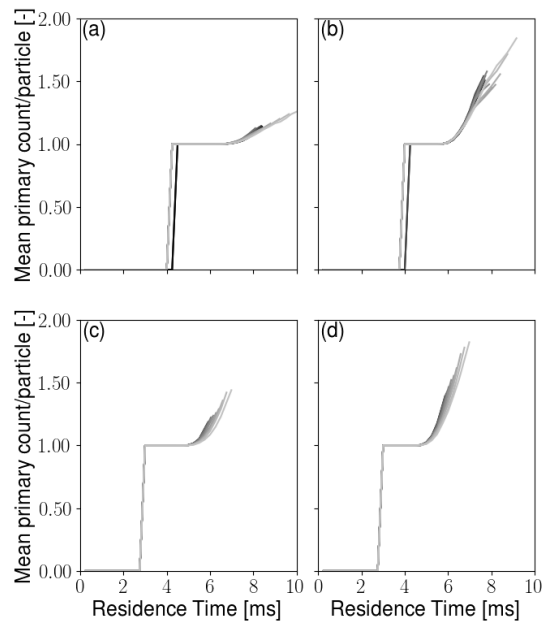
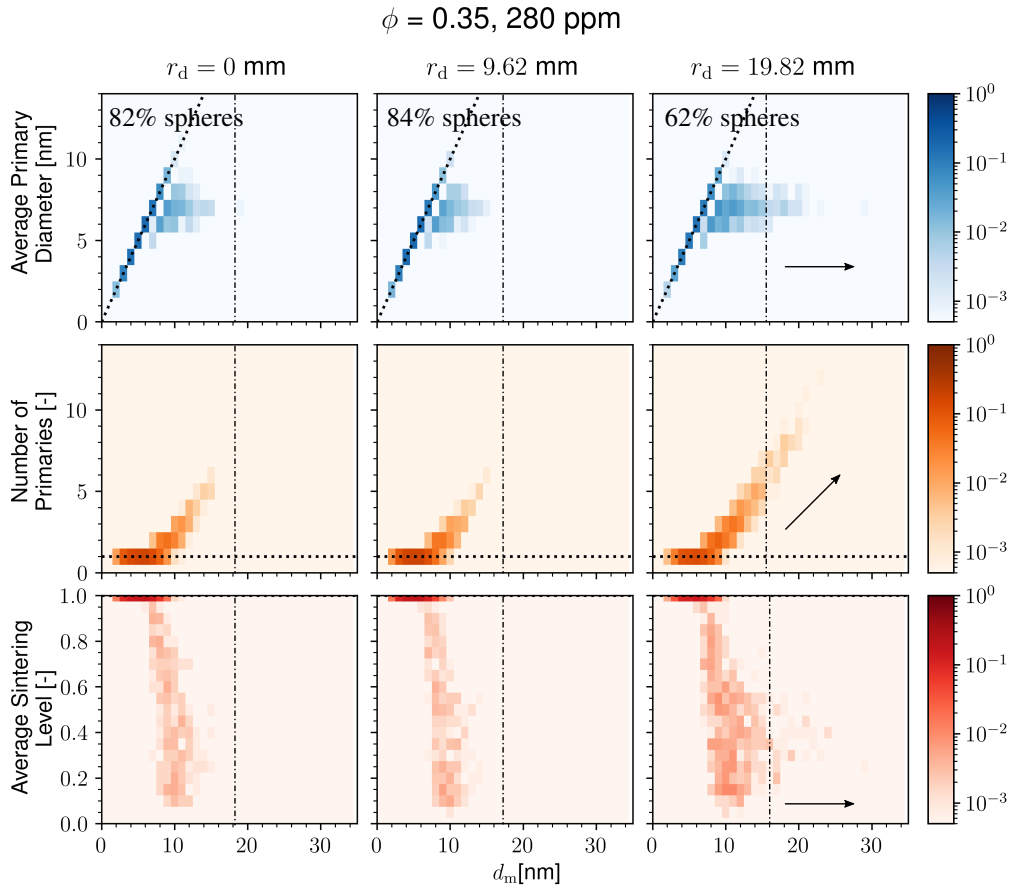
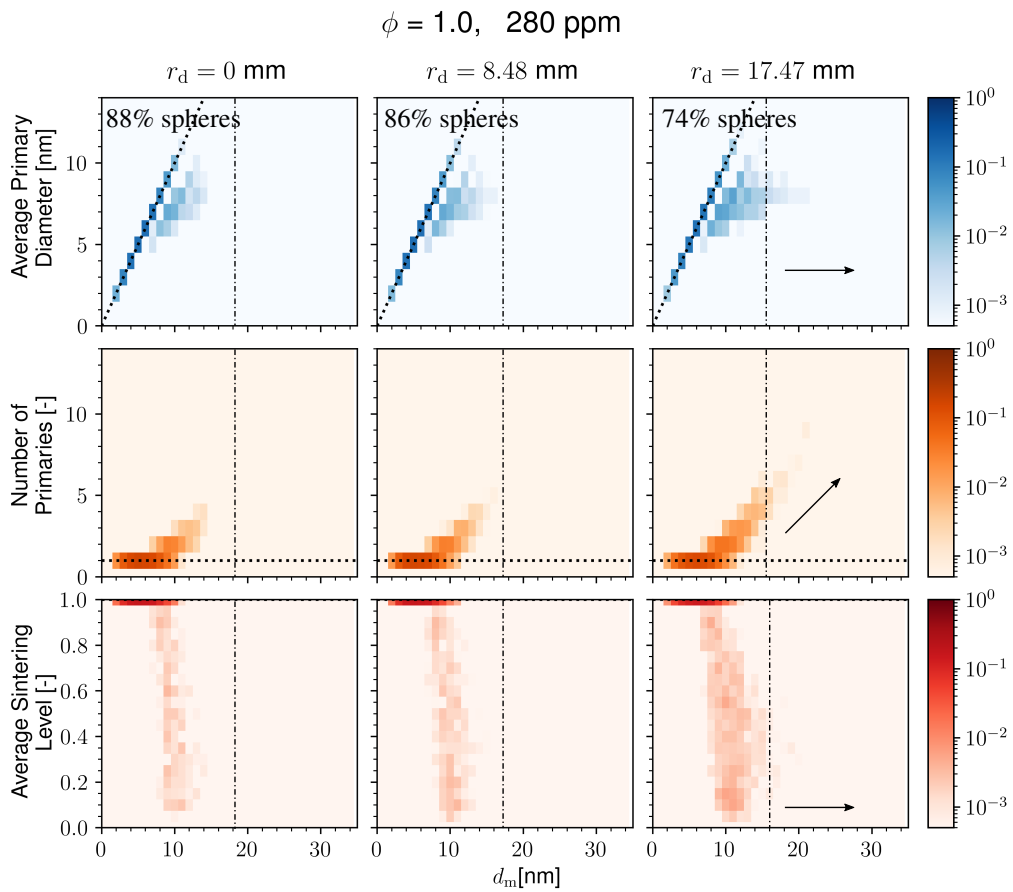


Figure C.4: Mean number of primaries per aggregate as a function of residence time along different trajectories (dark to light moving radially outwards from the centre of the flame) in (a) $\phi = 0.35$, 280 ppm flame, (b) $\phi = 0.35$, 560 ppm flame, (c) $\phi = 1.0$, 280 ppm flame, and (d) $\phi = 1.0$, 560 ppm flame.



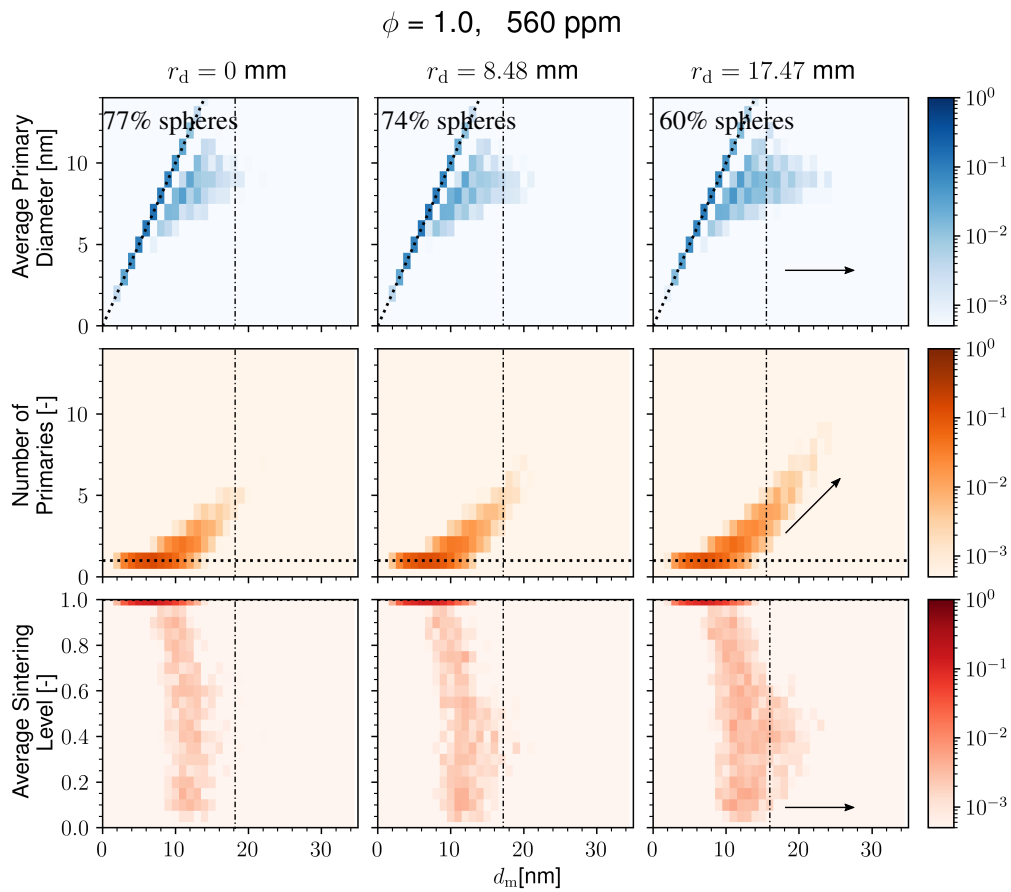
(a) Part 1: Lean flame with 280 ppm TTIP.

Figure C.5: Joint distributions of average primary diameter, number of primaries, and average sintering level with mobility diameter at different deposition radii, r_d . The averages are arithmetic means are taken over the primary particles within each aggregate. The fraction of particles that are spherical are reported as a percentage. The dotted black line corresponds to spherical particles, while the dot-dash lines mark the mobility diameter of large aggregates that form at large deposition radii.



(b) Part 2: Stoichiometric flame with 280 ppm TTIP.

Figure C.5: Cont.



(c) Part 3: Stoichiometric flame with 560 ppm TTIP.

Figure C.5: Cont.

References

- [1] P. Atkins. *Physical Chemistry*. W. H. Freeman, 2006. ISBN 0716787598.
- [2] R. B. Bird, W. E. Stewart, and E. N. Lightfoot. *Transport Phenomena*. John Wiley & Sons, 2nd edition, 2001.
- [3] P. Buerger, D. Nurkowski, J. Akroyd, S. Mosbach, and M. Kraft. First-Principles Thermochemistry for the Thermal Decomposition of Titanium Tetraisopropoxide. *J. Phys. Chem. A*, 119(30):8376–8387, 2015. doi:10.1021/acs.jpca.5b01721.
- [4] CMCL Innovations, UK. *kinetics[®] and SRM Engine Suite*, v9.1.1, 2019. URL <https://cmclinnovations.com>.
- [5] M. Frenklach. Method of moments with interpolative closure. *Chem. Eng. Sci.*, 57(12):2229–2239, 2002. doi:10.1016/S0009-2509(02)00113-6.
- [6] M. Frenklach and S. J. Harris. Aerosol dynamics modeling using the method of moments. *J. Colloid Interface Sci.*, 118(1):252–261, 1987. doi:10.1016/0021-9797(87)90454-1.
- [7] S. K. Friedlander. *Smoke, Dust and Haze*. Oxford University Press, Oxford, second edition, 2000.
- [8] S. Gordon and B. J. McBride. Computer program for calculation of complex chemical equilibrium compositions, rocket performance, incident and reflected shocks and chapman-jouguet detonations. Technical Report NASA Report SP-273, National Aeronautics and Space Administration, Washington, DC, United States, March 1976. URL <https://ntrs.nasa.gov/archive/nasa/casi.ntrs.nasa.gov/19780009781.pdf>.
- [9] J. O. Hirschfelder and C. F. Curtiss. The Theory of Flame Propagation. *J. Chem. Phys.*, 17(11):1076–1081, 1949. doi:10.1063/1.1747115.
- [10] J. O. Hirschfelder, C. F. Curtiss, and D. E. Campbell. The theory of flame propagation. iv. *J. Phys. Chem.*, 57(4):403–414, 1953. doi:10.1021/j150505a004.
- [11] J. O. Hirschfelder, C. F. Curtiss, and R. B. Bird. *Molecular Theory of Gases and Liquids*. John Wiley & Sons, 2nd edition, 1954.
- [12] J. L. Hodges. The Significance Probability of the Smirnov Two-Sample Test. *Arkiv för Matematik*, 3(5):469–486, 1958. doi:10.1007/BF02589501.
- [13] R. Issa. Solution of the implicitly discretised fluid flow equations by operator-splitting. *J. Comput. Phys.*, 62(1):40–65, 1986. doi:10.1016/0021-9991(86)90099-9.
- [14] C. S. Lindberg, M. Y. Manuputty, P. Buerger, J. Akroyd, and M. Kraft. Numerical simulation and parametric sensitivity study of titanium dioxide particles synthesised in a stagnation flame. *J. Aerosol Sci.*, 138:105451, 2019. doi:10.1016/j.jaerosci.2019.105451.

- [15] M. Y. Manuputty, J. Akroyd, S. Mosbach, and M. Kraft. Modelling TiO₂ formation in a stagnation flame using method of moments with interpolative closure. *Combust. Flame*, 178:135–147, 2017. doi:10.1016/j.combustflame.2017.01.005.
- [16] F. J. Massey. The Kolmogorov-Smirnov Test for Goodness of Fit. *J. Am. Stat. Assoc.*, 46(253):68–78, 1951. doi:10.1080/01621459.1951.10500769.
- [17] S. Mathur, P. Tondon, and S. Saxena. Thermal conductivity of binary, ternary and quaternary mixtures of rare gases. *Mol. Phys.*, 12(6):569–579, 1967. doi:10.1080/00268976700100731.
- [18] L. Monchick and E. A. Mason. Transport Properties of Polar Gases. *J. Chem. Phys.*, 35(5):1676–1697, 1961. doi:10.1063/1.1732130.
- [19] T. Poinso and D. Veynante. *Theoretical and Numerical Combustion*. by the authors, third edition, 2012.
- [20] The OpenFOAM Foundation Ltd. OpenFOAM v5, 2017.
- [21] H. K. Versteeg and W. Malalasekera. *An Introduction to Computational Fluid Dynamics: The Finite Volume Method*. Pearson Education Ltd, Harlow, England ; New York, 2nd ed edition, 2007.
- [22] P. Virtanen, R. Gommers, T. E. Oliphant, M. Haberland, T. Reddy, D. Cournapeau, E. Burovski, P. Peterson, W. Weckesser, J. Bright, S. J. van der Walt, M. Brett, J. Wilson, K. Jarrod Millman, N. Mayorov, A. R. J. Nelson, E. Jones, R. Kern, E. Larson, C. Carey, Í. Polat, Y. Feng, E. W. Moore, J. Vand erPlas, D. Laxalde, J. Perktold, R. Cimrman, I. Henriksen, E. A. Quintero, C. R. Harris, A. M. Archibald, A. H. Ribeiro, F. Pedregosa, P. van Mulbregt, and Contributors. SciPy 1.0: Fundamental Algorithms for Scientific Computing in Python. *Nat. Methods*, 17:261–272, 2020. doi:10.1038/s41592-019-0686-2.
- [23] C. Wilke. A viscosity equation for gas mixtures. *J. Chem. Phys.*, 18(4):517–519, 1950. doi:10.1063/1.1747673.
- [24] F. Williams et al. Chemical-kinetic mechanisms for combustion applications, 2005. San Diego Mechanism web page, Mechanical and Aerospace Engineering (Combustion Research), University of California at San Diego <http://combustion.ucsd.edu/> (2005).